Research Article

Efficient phosphate removal from contaminated water using functional raw dolomite powder

George M. Ayoub[1] · Houri Kalinian[1] · Ramez Zayyat[1]

Abstract

Phosphate, when present in water, forms one of the basic nutrients that lead to eutrophication and its associated negative impacts. The use of raw dolomite powder as an adsorbent was found to be very effective in the removal of phosphates from various waters and wastewater matrices. Ayoub and Kalinian (Water Environ Fed 78:353–361, 2006) reported phosphate removals, amounting to 100%, over more than 300 bed volumes at inflow concentrations between 0.30 and 0.40 mg/L. This marked achievement led to the present study with the objective of defining the effects of the various parameters involved in the process and determining the optimal operating condition to achieve effective and sustainable removal efficiencies. Experimental work was conducted by passing three types of influent water and two types of wastewater jacked with a phosphate salt (KH_2PO_4) through a fluidized column bed of dolomite powder, where the effect of various parameters, including system operation mode, adsorbent particle size, rate of flow through the bed (contact time), initial phosphate concentration, influent pH, and the presence of competing anionic solutes on the adsorption of phosphate was evaluated. The results asserted that the most effective mode of operation for the system was the fluidized bed configuration. Results further showed that the smaller-sized dolomite powder (< 0.074 mm) sustains better adsorption. Also, higher contact time and lower feed phosphate concentration result in increased adsorption. Adsorption capacity was found to decrease with increased influent pH values. Competitive adsorption with existing anions was noted to occur, leading to reduced efficiency in phosphate removal. The Thomas and Yoon–Nelson models were deemed to agree best with the experimental data, while the Thomas model was determined to be the most descriptive of the column runs and to produce the most accurate predictive results. The use of dolomite as an adsorbent in the removal of phosphates, considering its wide availability, ease of application and regeneration capability, if operated under optimal conditions as determined by the present study, will present a highly sustainable process with added advantages over the more complex and costly adsorbents.

Keywords Dolomite · Phosphate · Adsorption · Process variables · Fluidized bed

1 Introduction

Phosphate release into surface waters, from point and diffuse sources, contributes to eutrophication problems in lakes and rivers characterized by excessive growth of algae and aquatic plants [2]. Effluent discharges with low concentrations of phosphates (< 0.1 mg/L) have been reported to induce eutrophication [3]. Conventional phosphorous removal technologies include the utilization of a variety of chemical and biological processes. Recent studies on biological technologies targeting the removal of phosphates from aqueous solutions reported on the use

Electronic supplementary material The online version of this article (https://doi.org/10.1007/s42452-019-0833-5) contains supplementary material, which is available to authorized users.

✉ George M. Ayoub, gayoub@aub.edu.lb | [1]Department of Civil and Environmental Engineering, American University of Beirut, Beirut, Lebanon.

SN Applied Sciences (2019) 1:802 | https://doi.org/10.1007/s42452-019-0833-5

Received: 22 May 2019 / Accepted: 24 June 2019 / Published online: 28 June 2019

of engineered environmental bacteria [4] and specifically grown bacterial consortia in biofilm bioreactors [5], as well as on the introduction of shifts in structure and functions of microbial communities [6]. Studies also reported on the introduction of supplemental materials [7, 8] or specific bacterial species [9] to activated sludge aerobic reactors that enhanced phosphates removal.

Concurrently, work on chemical technologies covered a wide range of processes that included coagulation/flocculation and more recently electrocoagulation [10], adsorption in which a wide number of chemicals were proposed in the application of these processes. In this context, metallic nanoparticles and nanocomposites were extensively investigated [11, 12] as well as iron and its compounds [13, 14]. Applications using aluminum and magnesium in various forms were also studied [12, 15, 16]. Zeolites [17, 18] and silicates [19, 20] as well as other materials such as activated red mud [21], coal gangues [22] and chitosan [23, 24] were reported to be effective adsorbents. Sewage sludge-based adsorbents were also shown to have a good adsorbing potential [4, 25]. A variety of composite materials have also shown promise in phosphate removal [26, 27]. Most of these reported studies were adsorption-related studies due to the advantages that have been demonstrated to exist over the coagulation/flocculation processes.

Biological processes, on the one hand, fall short of achieving removal levels that are commensurate with the stringent standards imposed, while chemical processes, related to coagulation and electrocoagulation, entail excessive chemical use and hence excessive production of sludge associated with complexity in operation and high operating cost [28, 29]. Novel methods such as the use of adsorbents, as noted earlier, have been introduced to alleviate these problems by achieving close to complete phosphorous removal without the excessive use of chemicals and consequently without the production of sludge.

Major factors affecting the extent of phosphorus adsorption to an adsorbent include chemical adsorbate characteristics and intrinsic adsorbent characteristics such as pore size, particle density, permeability and surface area. Other factors include particle size, temperature, pH of solution, contact time, initial concentration of phosphate, and presence of competing solutes that reduce available adsorption sites by inorganic salts which have been reported earlier by Cheremisinoff [30] and Lee et al. [31] and more recently by Chen et al. [32], Kang et al. [19] and Awual [26, 33].

Raw dolomite powder, obtained from crushed dolomitic rock, was found to be a very effective adsorbent for removing low concentrations of phosphates present in various water and wastewater matrices [1]. Besides, it imposes a number of advantages when compared to the more complex and costly adsorbents reported in the literature in that it is highly sustainable, widely and easily available, enjoys simplicity in application, is easily reactivated, does not produce sludge, and is very efficient in removal of phosphates from aqueous solutions. Complete removal of phosphates was achieved over more than 300-bed volumes at input phosphorus concentrations ranging between 0.30 and 0.40 mg/L [1]. In determining the optimal conditions under which the dolomite will be most effective in achieving maximum removal levels, a number of parameters were evaluated in order to assess their effect on the efficiency of the process. Physical parameters such as system operation mode, adsorbent particle size, rates of flow through the bed (contact time), water quality and initial phosphate concentration were investigated. The effect of the use of dolomite on the quality of water and the presence of competing solutes were assessed. The results of the study are reported in this paper.

2 Materials and methods

2.1 Dolomite powder

The adsorbing material (dolomite powder) used in the removal of phosphorus from water and wastewater was obtained from crushed dolomite rock from the Sibline area, South of Beirut, Lebanon, which was found to have dolomitic formations [34]. Like with all mineral deposits, different characteristics are normally encountered. However, the main components that were of interest in this study were the predominant concentrations of calcium and magnesium oxides, which are considered to be the effective chemicals that will contribute to the treatment process. The chemical properties of the utilized dolomite powder as determined through X-ray diffraction are shown in Table 1.

Furthermore, ion chromatography was adopted in determining specific constituents of the powder such as chlorides, sulfates and nitrates (Table 2).

The dolomite powder was prepared by crushing the pieces of the dolomite rock using a crushing machine at the Soil Mechanics Laboratory. Sieving was conducted for the powder dolomite after crushing to classify the size distribution of the powder particles based on ASTM standard analysis. The sizes of the standard mesh sieves used ranged from number 80 to 200, i.e., 0.177 to 0.075 mm. The dolomite powder that passed the 200-mesh sieve (< 0.075 mm) was selected to be the optimal dolomite size to be used in the experimental work. The resulting physical properties of the powder are shown in Table SM1. In addition, the particle size distribution of the selected sieved powder was determined by the hydrometer method [35]

Table 1 Chemical composition of the collected dolomite rock

Compound	Percent composition[a] (%)
SiO_2	0.77
Al_2O_3	0.14
Fe_2O_3	0.19
CaO	30.85
MgO	21.55
K_2O	0
TiO_2	0.09
P_2O_5	0
Loss on ignition	46.26

[a]Analyzed at the Sibline factory laboratory, average of two readings

Table 2 Average anion concentrations of powder dolomite sample

Parameter	Concentration[a] (mg/Kg)
Chloride	121
Nitrate	48
Sulfate	268

[a]Average of two readings

and is presented in Table SM2. The resulting powder was stored for later use in the experiments.

2.2 Testing setup and procedure

Various experimental procedures were first examined in order to determine the optimal setup to be adopted in conducting the study. These procedures included the jar-test setup, the fixed-bed continuous down-flow setup and the up-flow fluidized bed setup. The results of the jar test showed unsatisfactory phosphate removal efficiencies, while the fixed-bed down-flow model was found unsuitable because of flow permeability and clogging problems. To alleviate this issue, a mixed sand and dolomite powder bed were also investigated; however, a channeling problem was encountered in this case which resulted in low phosphate removal levels. The up-flow model was found to be the most feasible of the three tested procedures as it resolved most of the problems associated with the jar test and the down-flow models. Consequently, the fluidized bed setup was selected for the testing procedures. The experiments were conducted using two 1.5-cm-diameter, 120-cm-long glass columns packed with dolomite powder (Fig. 1). The backflow velocity was selected to fluidize the bed and yet not reach the terminal velocity. A peristaltic

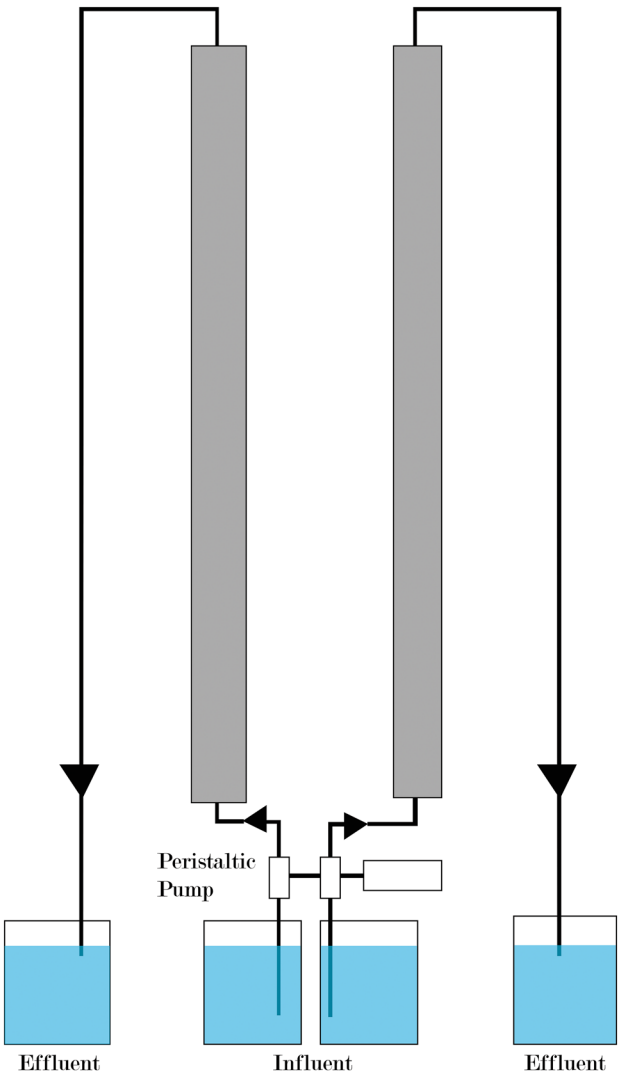

Fig. 1 Experimental setup

pump (Masterflex, Cole Palmer) was used to feed the solution through the bed. The bed consisted of 28.53 g of dolomite powder packed to a depth of 10 cm. The resulting volume of the bed was 16 ml with a 5-ml pore volume. Preliminary tests indicated the permeability issues to have been eliminated, and an enhanced contact between the influent and the powder volume was achieved. Furthermore, good phosphate removals were attained coupled with easier operation and control of the setup.

Series of experiments were conducted employing various flow rates, ranging from 5 to 10 ml/min (1.7 $m^3/m^2/h$ and 3.4 $m^3/m^2/h$, respectively), to assess the dynamic effect of the different flow rates (contact time) on the removal efficiency. The effect of particle sizes on removal efficiency was also evaluated employing identical adsorbent doses (28.53 g) and maintaining similar test conditions such as flow rate (5 ml/min) and type of

influent, distilled water (DW). Initial phosphate concentrations ranged from 0.75 to 1.1 mg PO_4/L. Dolomite sizes employed ranged from particles greater than 0.177 mm to particles smaller than 0.074 mm, denoted by mesh sizes > 80 and < 200, respectively.

2.3 Test feed samples

For the assessment of the impact of feed water characteristics on adsorption, three different influent waters, namely distilled water (DW), synthetic ground water (SGW), and tap water (TW), and two secondary-treated sewage effluents (STSE) were used in the testing activity.

Specific amounts of phosphate salt (KH_2PO_4) were used in the preparation of the influent solutions using DW and TW, while SGW was prepared by adding 35 mg $MgSO_4{\cdot}7H_2O$, 12 mg $CaSO_4{\cdot}2H_2O$, 12 mg $NaHCO_3$, 6 mg NaCl and 6 mg KMO_3 to 1 L DW into which a fixed amount of KH_2PO_4 was spiked. As for the chemically treated wastewater supernatants, STSE-B and STSE-L, these were the result of a bench-scale chemical precipitation treatment of raw sewage using standard jar-test apparatus (Phipps and Bird Inc., Model 300) with the application of liquid bittern and lime, respectively, and with NaOH used as the alkalizing agent. The pH of the tested influents was adjusted at 7.1–7.3 prior to starting the experiments. Table 3 depicts the characteristics of the test feed waters.

2.4 Testing procedures

To evaluate the adsorption efficiencies of phosphate by the adsorbent raw dolomite, four sets of experiments were conducted with each set being repeated at least twice. All tests were conducted at room temperature (22 ± 1 °C). The optimal test flow rate of 5 ml/min (1.7 $m^3/m^2/h$) and the dynamic effect on the removal efficiency were determined in the first set, while the second set dealt with determining the effect of dolomite particle sizes on the removal efficiency of phosphates. Table SM3 classifies the dolomite particle sizes indicated by the standard sieve numbers. Evaluating the adsorbate removals with varying initial influent concentrations at a constant size of < 200 mesh and flow rate of 5 ml/min was conducted in the third set, where different phosphate doses, that yielded concentrations ranging between 0.28 and 1.3 mg P–PO4/L, were spiked in the four influent samples. Finally, tests conducted in the fourth set covered an assessment of the efficacy of the feed water quality on the adsorption process. A summary of the experiments conducted is presented in Table SM4. This involved measuring variations in the physical and chemical characteristics of the effluents of the feed solutions by measuring pH, conductivity, total dissolved solids (TDS), orthophosphate, sulfate, magnesium, and calcium concentrations.

The effect of initial phosphate concentration on the process of adsorption was evaluated by conducting experiments with different initial phosphate concentrations using three types of influents: DW, SGW and TW.

Table 3 Average physicochemical composition of the test influents

Parameter	Influent type				
	DW	SGW	TW	STSE-B	STSE-L
pH	6.70	7.20	7.94	10.5	10.8
TDS, mg/L	72	78	257	4100	1980
Conductivity, µmhos/cm	145	157	515	8250	4050
SO_4^{2-}, mg/L	20	46	58	805	131
Cl^-, mg/L	30	40	214	4000	1500
Alkalinity, mg/L as $CaCO_3$	0	10	180	–	–
Ca hardness, mg/L as $CaCO_3$	10	20	180	–	–
Mg hardness, mg/L as $CaCO_3$	25	23	40	–	–

2.5 Analytical methods

Because of the clear effluents produced, no processing was needed before proceeding with the analysis. Acid wash followed by distilled water rinsing of borosilicate glassware was used throughout the testing procedure. All cleansing materials that could contaminate the assay with phosphate were avoided. Tests conducted on the physicochemical characterization of the effluent samples were in accordance with "Standard Methods for the Examination of Water and Wastewater" [36]. Orthophosphates and sulfates were determined based on HACH test manual procedures as approved by USEPA. Table SM5 presents the parameters, methods of analysis and instrumentation employed in the analysis.

2.6 Modeling breakthrough curves

Modeling of column behavior, as well as error analysis, was conducted for the effect of phosphate absorption with change in flow rates as well as dolomite particle size variation. Thomas, Bohart–Adams, and Yoon–Nelson models were used to model the behavior of uptake of phosphates on the dolomite columns. Bohart and Adams [37] reported that a model based on the surface reaction theory is considered to best describe the initial parts of sorption breakthrough curves [38]. The model is based on the equation [39]:

$$\ln\left(\frac{C_t}{C_o}\right) = k_{AB}C_0 t - k_{AB}N_0\frac{Z}{u_0} \quad (1)$$

where influent and effluent concentrations of phosphates are represented by C_o and C_t, respectively. k_{AB} (L/mg min) is the mass transfer coefficient, t (min) is the sample time, N_0 (mg/L) is the saturation concentration, U_0 (cm/min) is the

linear velocity calculated by dividing the flow rate by the column cross-sectional area, and Z (cm) is the bed depth [40, 41].

The Thomas model [42] is the most general and widely used model for expressing the theoretical behavior of adsorption column performances. The linearized form of the Thomas model is expressed as [43, 44]:

$$\ln\left(\frac{C_0}{C_t}-1\right)=\frac{K_{Th}q_0m}{Q}-K_{Th}C_0t \quad (2)$$

where Q (mL/min) is the volumetric flow rate, K_{Th} is Thomas kinetic coefficient, t (min) is the total flow time, q_0 and m (mg/g) are the adsorption capacity and mass of the adsorbent, respectively. The values for K_{Th} and q_0 were determined by plotting $\ln\left(\frac{C_0}{C_t}-1\right)$ versus t [45].

Yoon–Nelson model is a simpler model utilized for single-component systems, which assumes that the rate of decrease in the probability of adsorption for adsorbate is proportional to both the probability of adsorbate adsorption and the probability of adsorbate breakthrough on the adsorbent, and is given by the following [46, 47]:

$$\ln\frac{C_t}{C_0-C_t}=K_{YN}t-\tau K_{YN} \quad (3)$$

where K_{YN} is the rate constant, τ (min) is the time required for 50% adsorbate breakthrough, and t (min) is time of the run. Plotting $\ln\frac{C_t}{C_0-C_t}$ versus t K_{YN} and τ can be determined by using the slopes and intercepts of the regression equations obtained from the applied linear regression models.

3 Results and discussion

3.1 Effect of process variables on phosphate removal efficiency

3.1.1 Hydraulic flow rate/contact time

The effect of contact time on phosphates and other contaminants adsorption by a number of different adsorbents has been extensively studied [48–51]. Using batch experiments, Awual [26] studied the removal of phosphates using mesoporous silica and ligand embedded composite adsorbent over a reaction time of 10–90 min; it was observed that over 90% of the available phosphates were removed in the first 30 min, while the rest were removed over a more extended period of time (up to 90 min). The observation of fast adsorption was attributed to abundant protonated active sites combined with the highly ordered porous frameworks of composite adsorbent [52–54]. Using DW with the initial influent phosphate concentrations of 0.75 and 0.76 mg/L, the average phosphate removal efficiencies varied between 89, 84 and 90, 34% at the start and end of the experimental run (56 bed volumes) for the flow rates of 5 and 10 ml/min, respectively.

Figure 2 shows phosphate removal percentages versus number of beds at different flow rates. It is noted that fixation capacity is dependent on the hydraulic condition, which determines the contact time between the adsorbent (dolomite) and the adsorbate (phosphate) [55]. In this context, it is noted that adsorption capacity increases with the increase in contact time, i.e., lower flow rates. This substantiates earlier studies that reported increased adsorption rates with increased contact time using a variety of adsorbents [21, 56]. According to Xing et al. [56], adsorption of phosphates on activated siderite ore (ASO) increased with higher contact time, it was reported that adsorption equilibrium was reached after 8 h for most

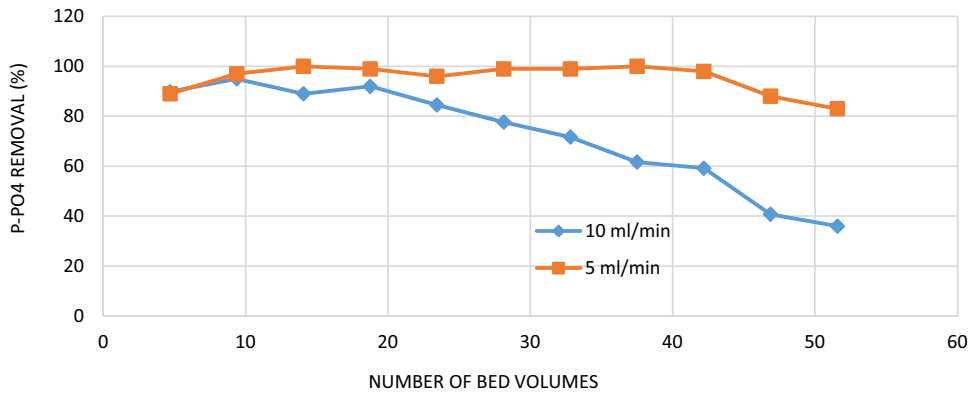

Fig. 2 Phosphate removal percentages as a function of flow rate

particle sizes, and adsorption capacity was achieved after 24 h for 0.05–0.1 mm particle size.

3.1.2 Size of dolomite particle

Figure 3 depicts the average percent phosphate removal for the various dolomite particle sizes as a function of number of bed volumes of effluent treated. The plot reveals that at the start of the experimental run phosphate removals attained were 97.0, 90.3, 77.2, 76.1 and 93.7 percent, and at the end of the run (52 bed volumes) percent phosphate removals achieved were in the range of 84.1, 63.4, 56.9, 46.6 and 35.5 percent for dolomite sizes of < 200, 200–140, 140–100, 100–80 and > 80, respectively. These results confirm higher phosphate removal efficiencies for smaller adsorbent size ranges. This increase in removal with decrease in particle size is attributed to the relatively larger surface areas and hence the higher number of available adsorption sites offered by the smaller particle sizes. Removal efficiencies were assessed based on the initial influent phosphate concentration. It was reported that the adsorption capacity of 2.5 mg/g of phosphates was achieved for the smallest particle size of ASO (0.05–0.1 mm), while under similar initial conditions, larger particle sizes (0.85–3.35 mm) exhibited an adsorption capacity of 1 mg/g [56].

3.1.3 Initial phosphate concentration

The effect of varying initial phosphate concentrations on removal is illustrated in Fig. 4. Higher percent sorption with decreasing initial concentration was found to be the governing trend. This pattern was noted with TW in which an increase in phosphate concentration from 0.340 to 1.113 mg/L led to a 25.7 percent reduction in removal efficiency. Contradicting results were obtained when using DW (0.283–0.977 mg/L) and SGW (0.335–0.845 mg/L) where the applied concentrations were more than doubled, and where removal efficiencies decreased by only 3.2 and 6.8 percent, respectively. This behavior tends to indicate that the initial phosphate concentrations used in this study had a minor effect on removal efficiencies, but rather the water quality and the presence of competing elements were the factors that played the more important role in removal efficiencies. In this context, it is noted that the presence of alkalinity in DW (0 mg/L) and SGW (10 mg/L) is practically negligible when compared to TW (180 mg/L). The possible presence of HCO_3^- ions could lead to the reduction of phosphate removal with increased influent phosphate concentrations as it is reported [56, 57] that HCO_3^- is highly competing ions when it comes to phosphate adsorption. It is, however, to be noted that the results obtained are not in agreement with the reported studies as these indicated an improvement in adsorption efficiency with increased initial phosphate concentration up to a certain concentration level beyond which no increase was detected [21].

3.1.4 Effect of pH on phosphate removal

It is well established that solution acidity is a controlling factor in adsorption processes, and it directly impacts ionic speciation and ionization state of the ions in aqueous media [58–61]. Studies on diverse absorbents have shown that the effect of surface charge of the adsorbents and the adsorbates dominates the adsorption capacity and determines the uptake of ions from the aqueous phase [33, 62, 63]. Figure 5 depicts phosphate removal capacities for tested samples with different pH values. It is evident from the descending curve arrived at, when measuring the number of bed volumes where phosphate removal attained 100% as a function of pH, that as pH increases removal decreases. This may be attributed to the loss of electrostatic attraction toward phosphate anions as

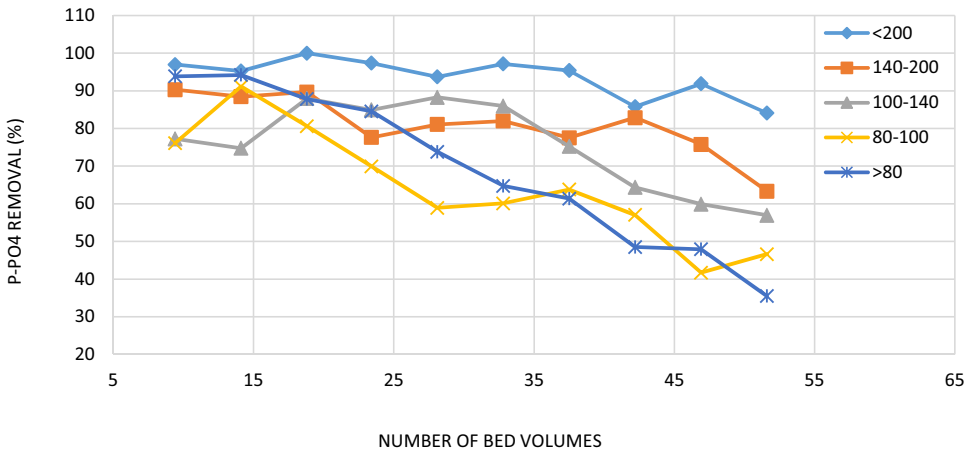

Fig. 3 Percent phosphate removal as a function of particle size range. (< 200 average of four tests), others (average of two tests each)

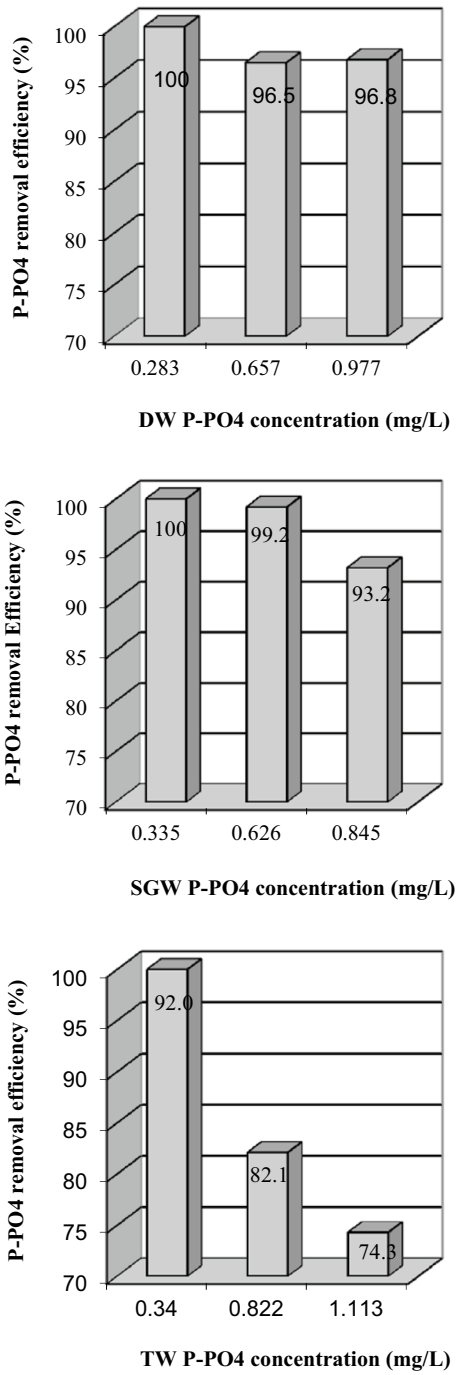

Fig. 4 Phosphate removal efficiencies in **a** DW, **b** SGW and **c** TW (over 47 bed volumes using various initial phosphate concentrations)

pH increases so do the negative charges which create a repelling force toward the anions. These results are in good agreement with recent studies where it was reported that phosphates can be removed by ASO in a relatively wide pH range between 3.0 and 11.0 [21, 56]. Awual [26] studied the effect of initial pH on the adsorption of phosphates using composite adsorbent, in the pH range of 3.0–7.0; the presence of monovalent $H_2PO_4^-$ and divalent HPO_4^{2-} as the major phosphate species leads to high adsorption values of phosphates; however, in the aforementioned study the optimal pH was selected to be in the neutral range of 7.0–9.0, where the divalent species HPO_4^{2-} is the most abundant species in the aqueous solution and was adsorbed in preference to competing species such as Cl^-, HCO_3^-, CO_3^{2-} and SO_4^{2-}. According to Helfferich [64], such an observation can be attributed to the effects of both electroselectivity and hydrogen bonding interactions [27]. Xu et al. [65] carried out a similar experiment using raw dolomite and calcite for the removal of phosphates, and the reported results suggest that the process of adsorption of phosphate on calcite and dolomite at pH 6.0–7.0 is mainly attributable to the precipitation of calcium phosphate complexes. It was also deduced that dolomite offers the strongest sorption capacity at increased pH levels of ≥ 8.0 when high phosphate concentrations are preset (> 200 mg/L). Karaca et al. [66] also stated that the polyprotic nature of phosphate molecules leads to a high pH dependency, and it was reported that phosphates bind with Ca^{2+} ions to from the adsorbent, and the high increase in pH of the aqueous solution lead to the formation of OH^- which competes with the PO_4^{3-} species lowering the adsorptive capacity of phosphates.

3.2 Physicochemical characteristics of column effluents

During the course of the experimental runs, effluent samples were collected at fixed time intervals and analyzed for physicochemical characterization. Parameters under assay included pH, conductivity, total dissolved solids (TDS), sulfate and phosphate. The different test influents (DW, TW, SGW and STSE) employed were repeatedly tested for the same parameters in an attempt to depict the effect of the dolomite bed on the final quality of the effluent.

3.2.1 Variation in pH

The pH of the different feed waters used during the experiments was noted to increase upon passing through the dolomite bed. The pH of the DW and SGW influents significantly increased from 7.2 and 7.3 to a pH of about 9.3. In contrast, a lower pH rise from about 7.3 and 7.5 to 8.03 and 8.4 was observed for the TW and STSE (STSE-B and STSE-L) influents, respectively. This is attributed to the buffering capacity of the TW and STSE influents. The rise in pH is attributed to the dissolution of the dolomite components, to yield free carbonates according to the reactions:

$$CaCO_3 \rightleftarrows Ca^{2+} + CO_3^{2-} \quad (4)$$

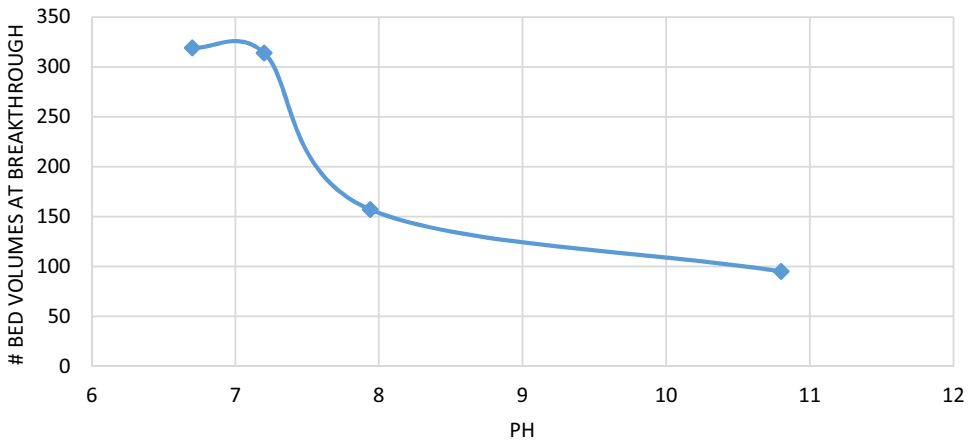

Fig. 5 Effect of pH on phosphate removal

$$MgCO_3 \rightleftarrows Mg^{2+} + CO_3^{2-} \quad (5)$$

The increase in pH value was noted to coincide with the liberation of calcium (Ca^{2+}) and magnesium (Mg^{2+}) ions into solution as discussed later. Figure 6 depicts average pH values attained with the different influents used.

The extent of pH rise was observed to be more significant with DW influents of lower initial pH values. While influent pH increased from 6.7 and 7.2 to 9.4 and 9.6, respectively, influents with initial pH of 7.8 demonstrated a final effluent pH of 8.9. However, this behavior was not maintained with TW influents where the degree of pH increase did not vary with varying initial influent pH.

3.2.2 Calcium and magnesium hardness

It was observed for all the experiments that the concentrations in Ca^{2+} and Mg^{2+} ions increased during the initial phase of the tests upon addition of dolomite and remained relatively constant thereafter. A significant release of Mg^{2+} ions into solution was manifested with the three DW, TW and SGW influents being tested. Magnesium hardness increased from 39, 23, and 31 to 61, 50 and 57 mg/L as CaCO3 for TW, SGW and DW, respectively (Fig. 7a). The increase in the magnesium hardness for all the influents was noted to be fairly constant varying between 22 and 26 mg/L as $CaCO_3$. On the other hand, increase in the concentration of Ca^{2+} ions is mostly prominent in the case of DW and SGW influents only; as for TW influents less significant Ca^{2+} releases were noted (Fig. 7b). Ca hardness increased from 20 and 33 to 40 and 47 mg/L as CaCO3 for SGW and DW influents, respectively. This was in contrast to the negligible Ca hardness increase from 178 to 180 mg/L as $CaCO_3$ for the TW influent followed by a mild decline in Ca concentration. This may be attributed to the initially high concentrations of bicarbonate ions (180 mg/L as $CaCO_3$) and calcium hardness (178 mg/L as $CaCO_3$) which renders further dissolution of $CaCO_3$ difficult to realize and the decline could be

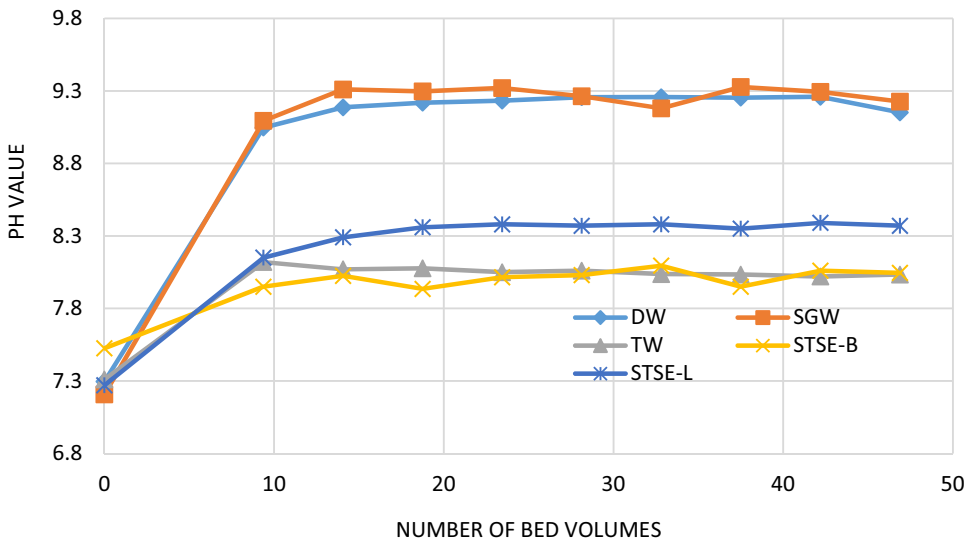

Fig. 6 Average effluent pH values attained with different influents

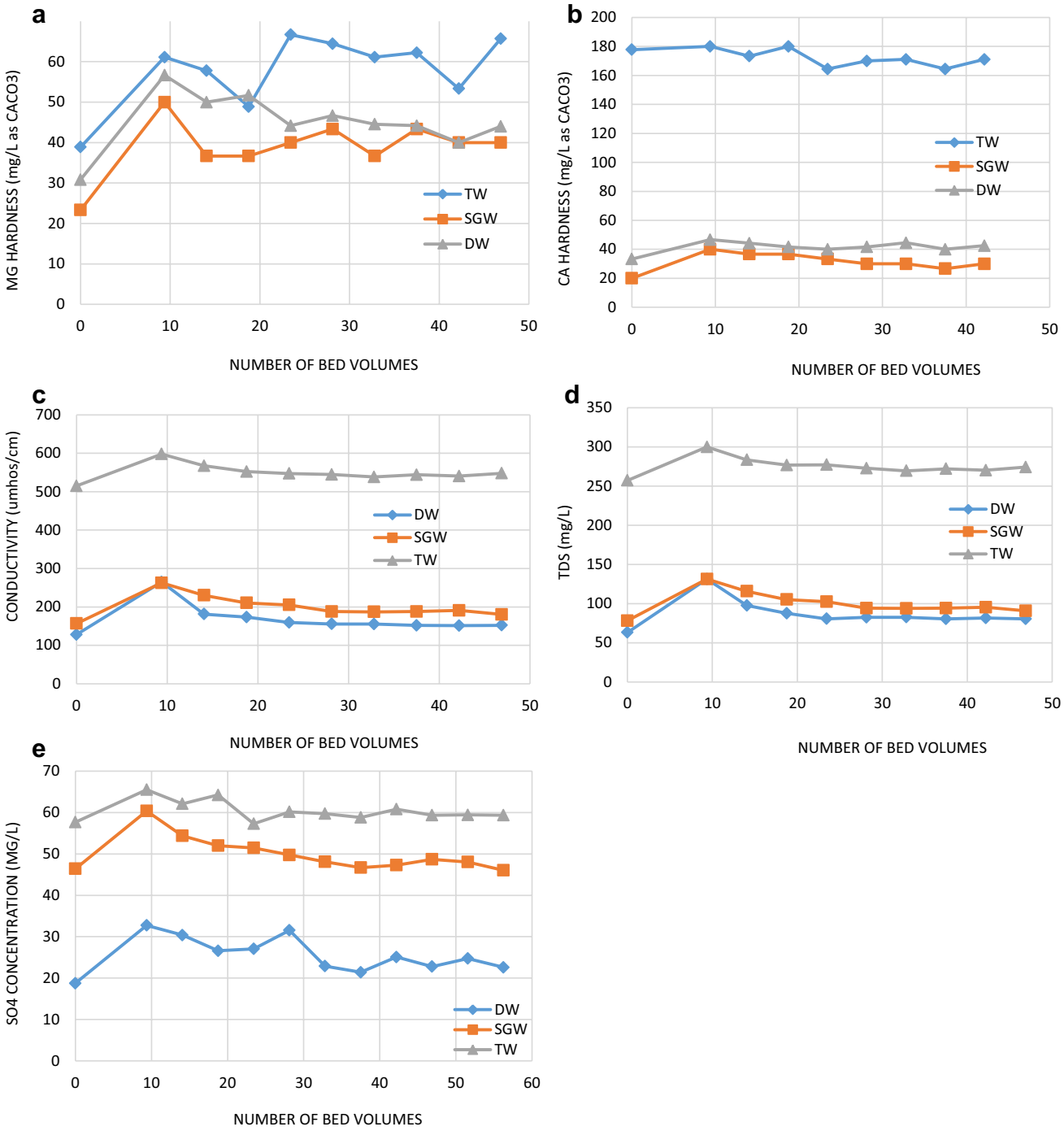

Fig. 7 Variation of concentrations for different influents: **a** Mg hardness, **b** Ca hardness, **c** conductivity, **d** total dissolved solids, **e** sulfates

attributed to $CaCO_3$ precipitation at the relatively high operating pH values.

3.2.3 Conductivity and TDS

Conductivity and TDS levels of the DW, SGW and TW influents increased from their initial values upon passage through the dolomite bed. A sudden upward incline followed by a slight decline in conductivity and TDS levels is attributed to the increase in the concentration of ions resulting from the dissolution of the dolomite bed components upon contact with the aqueous influents. Being prepared from raw rock material, the dolomite powder employed in the experimental runs showed

Table 4 Adams–Bohart, Thomas and Yoon–Nelson model parameters

	Adams–Bohart			Thomas			Yoon–Nelson		
	k_{AB} (L/mg min) × 10^{-3}	N_0 (mg/L)	R^2	K_{TH} (L/mg min) x 10^{-2}	q_0 (mg/g)	R^2	K_{YN} (L/min) x 10^{-2}	T (mg/g)	R^2
DW									
5 mL/min	62.3	8.3	0.59	10.8	11.2	0.84	8.1	42.5	0.94
10 mL/min	80.1	11.3	0.93	13.2	8.8	0.94	6.9	74.5	0.5
Sieve size									
> 80	39.7	5.4	0.98	11.5	2.7	0.85	8.6	20.8	0.85
80–100	19.5	7.7	0.78	6.8	1.7	0.79	5.1	12.8	0.79
100–140	21.7	9.1	0.96	5.2	3.2	0.93	3.9	24.5	0.93
140–200	12.8	41.5	0.49	3.7	4.6	0.82	1	3.8	0.44
< 200	8.9	22.5	0.58	1.9	8.0	0.81	1.1	68.0	0.58

Table 5 Absolute error function on the used models

Particle size	Thomas (δ)	Yoon–Nelson (δ)	Bohart–Adams (δ)
< 200	0.059	0.059	0.418
140–200	0.052	0.054	0.234
100–140	0.028	0.04	0.255
80–100	0.058	0.38	0.850
> 80	0.042	0.58	0.820

chloride, nitrate and sulfate ions in the range of 121, 48 and 268 ppm, respectively. The presence of ions in relatively considerable concentrations brought about a rise in conductivity and TDS values of the effluents produced. Figure 7c, d demonstrates conductivity and TDS levels of DW, SGW and TW influents, respectively. Being directly proportional to each other, conductivity and TDS values exhibited similar trends with all the test influents.

3.2.4 Competing effects of dissolved solutes on phosphate removal

The presence of anionic solutes such as chlorides, bicarbonates, nitrates and sulfates potentially competes with the targeted phosphate ions for sorption sites. Of these anions, sulfate ions are the candidate to produce the greatest suppression effect because they are divalent and thus possess a higher ionic charge. It is reported that sulfates compete with phosphate ions by reducing available adsorption sites through enhanced electrostatic interaction [67]. Based on this rationale, only the effect of sulfate on the fixation mechanism was considered in the study. However, with a dolomite sulfate impurity of about 268 ppm, fluctuations in the influent sulfate concentration during the experimental runs were totally masked. Measurements of sulfate concentration at 9.4 bed volumes (the first measured sample) showed significant increase in the concentration of the divalent ion in DW, SGW and TW from 19, 46 and 58 mg SO_4/L to 33, 60 and 66 mg SO_4/L, respectively. This increase was considered to be due to the washout of sulfate initially present in the dolomite as influent passed through the dolomite bed. Effluent measurements taken at sampling points and at the end of the experimental run (56.3 bed volumes) (Fig. 7e) demonstrated decrease in the sulfate ion concentration in DW, SGW and TW to end at values very close to the original concentration of 23, 46 and 59 mg/L, suggesting limited fixation of sulfate ions compared to the remaining anions. The competing effect of the anions present in the influent water is well depicted from the phosphate removal efficiencies as presented in Fig. 4. Referring to the anionic concentrations present in TW (58 mg/L, 214 mg/L and 180 mg/L for SO_4^{2-}, Cl^- and HCO_3^- expressed as $CaCO_3$, respectively) compared to SGW (46 mg/L, 40 mg/L and 10 mg/L respectively) and DW (20 mg/L, 30 mg/L and 0 mg/L, respectively), the results show proportionally reduced removals with higher ionic concentrations (TW > SGW > DW) and increase in applied phosphate concentrations. It is to be noted that the reported studies [56, 57] indicate that out of the cations in the form of Cl^-, NO_3^-, NO_2^-, SO_4^{2-}, and HCO_3^- only HCO_3^- has shown to possess a competitive adsorption potential to phosphate. In addition, it is to be noted that this potential is a function of the concentration of the anions present where the higher the concentration, the more effective the competing activity as demonstrated in this study.

3.3 Regeneration of dolomite bed

Three attempts were conducted at determining the most effective method to achieve desorption of phosphate from the dolomite surface, which included the application of an

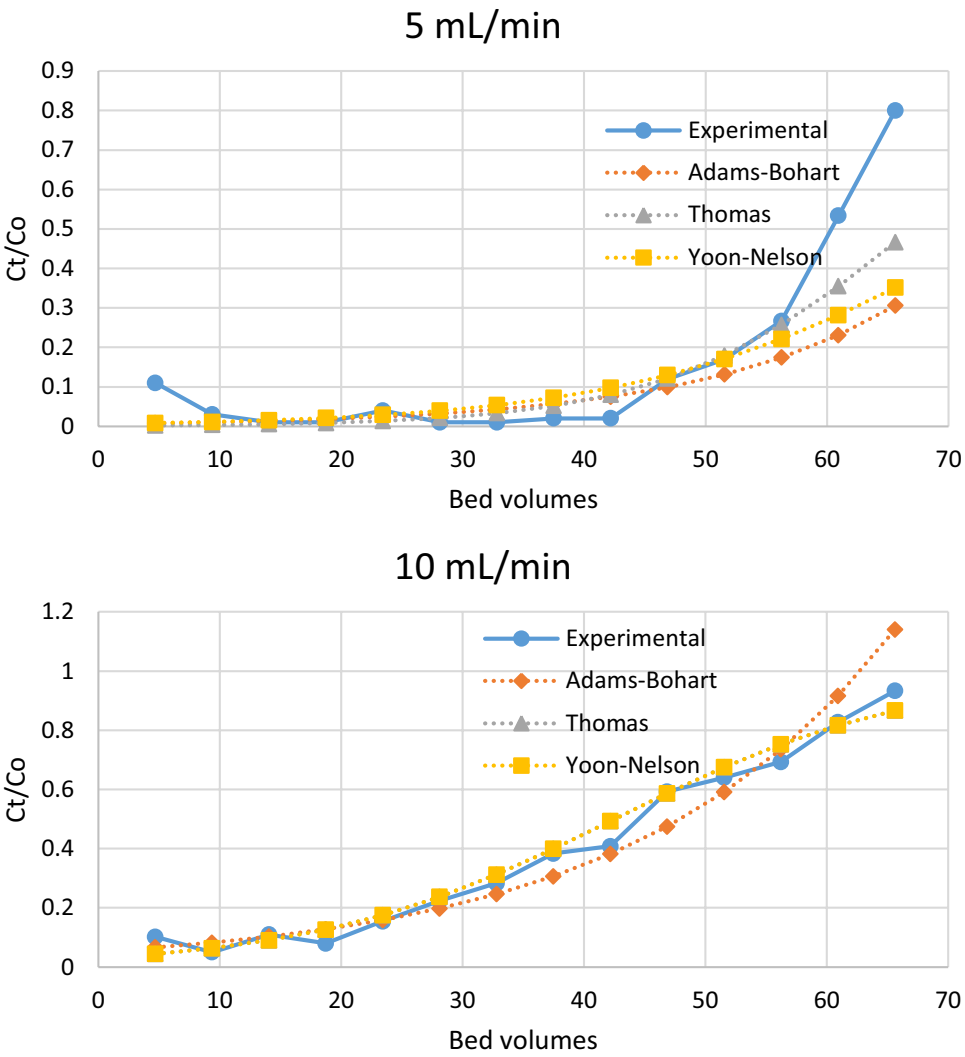

Fig. 8 Experimental versus predictive (DW 5 and 10 mL/min)

acid, distilled water, and a base. The latter method was found to produce the best results. This method included the application of a NaOH solution diluted to a pH of 10.5. The results indicated appreciable elution of the phosphate; however, a high volume of the solution was needed to achieve near-complete desorption. Figure SM1 depicts the three cycles of the test which included adsorption, desorption and re-adsorption. It is to be noted that the test was conducted with an influent of a relatively high concentration of phosphate (1.87 mg/L) relative to 0.3–0.4 mg/L of phosphate concentration used in the original experimental study, a condition which elucidates the relatively fast exhaustion of the bed.

3.4 Breakthrough curve modeling results

Applying Adams–Bohart model on the reported data, the respective values of N_0 and k_{AB} were calculated and are presented in Table 4. Observed values of k_{AB} increased with an increase in flow rate and particle sizes with R^2 ranging from 0.49 to 0.93. These results are in agreement with Guibal et al. [68] and Sekhula et al. [69] who stated that overall system kinetics may be influenced by external mass transfer, particularly in the initial part of adsorption in the column. The R^2 values for the Thomas model ranged from 0.79 to 0.94 indicating good linearity. Thomas model depicted the best R^2 value among the used models, indicating that this model best describes the breakthrough (Table 4). Results indicate that K_{TH} increases with increased flow rate and particle size, while q_0 decreases with increase in flow and increases with the decrease in particle size. Yoon–Nelson parameters K_{YN} and τ increased with increase in flow rate, and R^2 values ranged between 0.44 and 0.94 (Table 4).

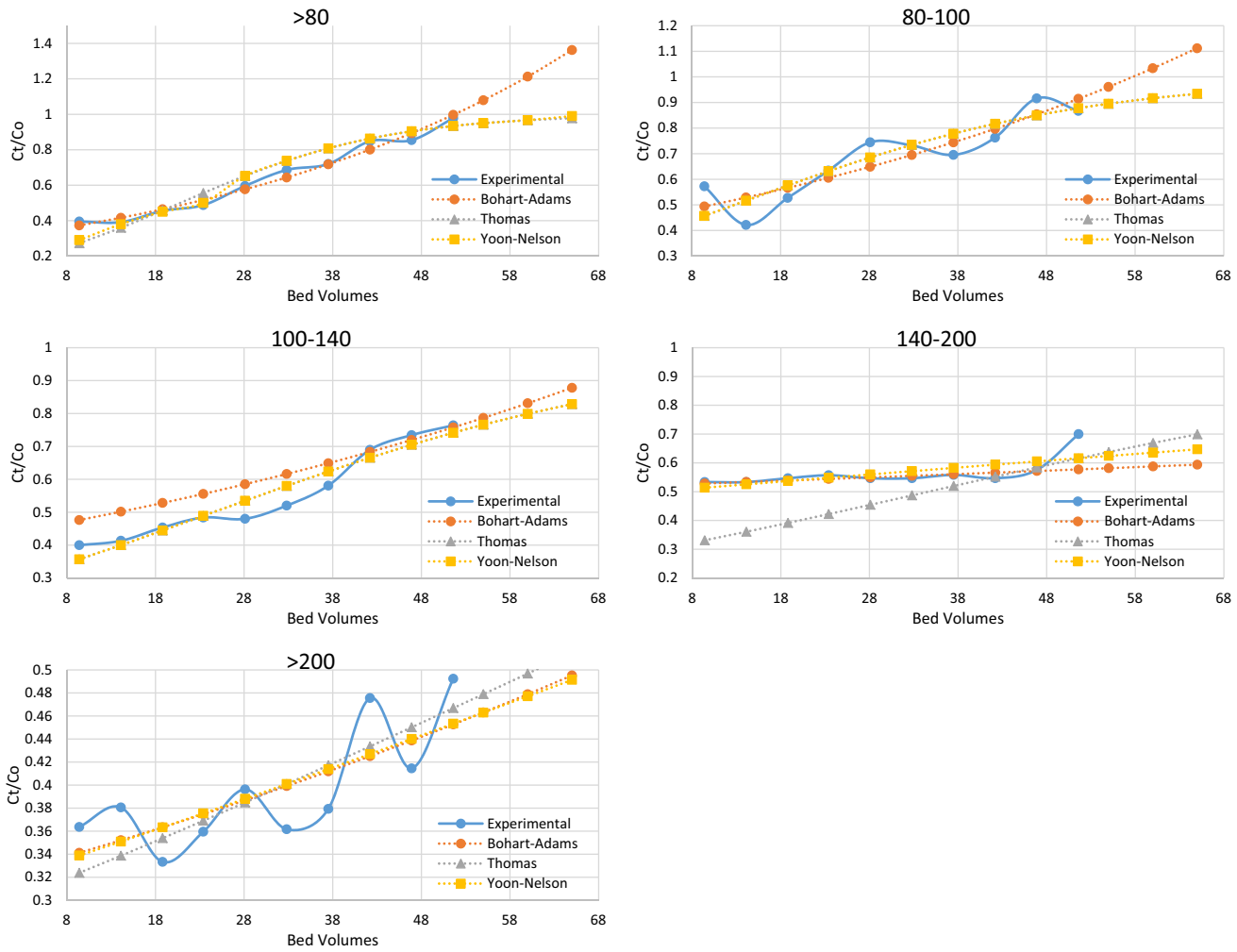

Fig. 9 Experimental versus predictive (particle size)

3.5 Error analysis

R^2 values calculated from the models indicate that Thomas model best fits the experimental data, closely followed by Yoon–Nelson, with Adams–Bohart showing the lowest R^2. For further confirmation, the formula used by Ghribi and Chlendi [70] was applied:

$$\delta = \sqrt{\frac{\sum \left(\frac{C}{Co}\right)_{cal} - \left(\frac{C}{Co}\right)_{exp}}{N}} \quad (6)$$

where N is the number of observations, $(C/Co)_{cal}$ is the ratio of effluent to influent phosphates concentrations as determined by applying the three models. $(C/Co)_{exp}$ is the ratio of effluent to influent phosphate concentrations obtained from experimental data. Table 5 represents the calculated error functions for the respective models.

Predictive vs experimental data for both DW at two different flows and various particle sizes are shown in Figs. 8 and 9. The deduction reached from comparing the models at hand is that the Thomas and Yoon–Nelson best describe the experimental curve throughout the plot; Bohart and Adams describes only the initial part of the curve and tends to deviate from the experimental data at later stages. The plots show that the predicted Thomas and Yoon–Nelson curves are extremely close to the experimental data curve and to one another.

4 Conclusions

This study aims at determining the optimal conditions under which the dolomite will be most effective in achieving maximum removal levels. For this purpose, a number of physical parameters such as system operation mode, adsorbent particle size, rates of flow through the

bed (contact time), water quality and initial phosphate concentration were investigated. The fixation capacity of dolomite was noted to be dependent on the hydraulic conditions at which the system was operated. Higher removal efficiencies were attained with lower influent feeding flow rates due to longer contact time between the adsorbent (dolomite) and the adsorbate (phosphate). The effect of dolomite particle size and initial phosphate concentrations was determined to be significant factors in the performance of the process and hence the effluent quality produced. Phosphate adsorption followed the general pattern of higher percent sorption with smaller dolomite size ranges and decreased the initial phosphate concentrations. The effect of altering the initial pH of the aqueous solution was proved to be a controlling factor in the removal of phosphates. At acidic pH levels, monovalent H_2PO^{4-} and divalent HPO_4^{2-} were present in the aqueous phase and were subsequently adsorbed on the dolomite sites; however, an increased adsorption was noted at neutral pH levels which was attributed to the abundant presence of divalent species HPO_4^{2-} which was thought to be adsorbed in preference to competing anions such as sulfates, chlorides and bicarbonates. On that note, the competing effect of the anions present in the influent water was apparent when using TW and SGW exhibiting a higher concentration of competing anions than that of DW. The results show proportionally reduced removals of phosphates on dolomite columns with higher ionic concentrations (TW > SGW > DW) and increase in applied phosphate concentrations.

During the course of the study, assessment of the physicochemical characteristics of the column effluents revealed a significant increase in the pH value of components to yield carbonates of calcium and magnesium responsible for the high pH levels. On the other hand, only a slight pH rise was observed for the TW and STSE influents due to their buffering capacity. Releases of Mg^{2+} and Ca^{2+} ions were observed to coincide with the increase in the conductivity and TDS levels of the effluents. The upward incline of these parameters is attributed to the dissolution of the dolomite bed components upon contact with the aqueous influents. Successful regeneration was found to occur through the application of NaOH solution diluted to a pH of 10.5. Modeling was carried out to further explain the behavior of phosphates upon exposure to the dolomite bed; as a result, both Thomas and Yoon–Nelson models agreed with the experimental data. The Bohart–Adams model deviated from the experimental data with time. Error analysis showed the Thomas model to be the most descriptive of the column runs, and the absolute error analysis indicated that Thomas model produced the most accurate predictive results.

Finally, it is to be noted that when raw dolomite, which offers a low cost, naturally and widely available material, is to be used as an adsorbent for phosphate removal from aqueous solutions using column applications; the optimal process should incorporate a fluidized bed with milli-sized particles operating under neutral pH and relatively low flows.

Acknowledgements The facilities of Environmental Engineering Research Center at AUB were used to conduct the study and accordingly are acknowledged herein.

Compliance with ethical standards

Conflict of interest The authors declare that they have no conflict of interest.

References

1. Ayoub GM, Kalinian H (2006) Removal of low-concentration phosphorus using a fluidized raw dolomite bed. Water Environ Res 78:353–361
2. Carpenter S, Caraco NF, Correll DL, Howarth R, Sharpley AN, Smith V (1998) Non-point pollution of surface waters with phosphorus and nitrogen. Ecol Appl 8:8–9. https://doi.org/10.2307/2641247
3. Yang XE, Wu X, Hao HI, He ZI (2008) Mechanisms and assessment of water eutrophication. J Zhejiang Univ Sci B 9:197–209. https://doi.org/10.1631/jzus.B0710626
4. Wang J, Tong X, Wang S (2018) Zirconium-modified activated sludge as a low-cost adsorbent for phosphate removal in aqueous solution water. Air Soil Pollut 229:47. https://doi.org/10.1007/s11270-018-3704-6
5. Saha A et al (2018) Simultaneous sequestration of nitrate and phosphate from wastewater using a tailor-made bacterial consortium in biofilm bioreactor. J Chem Technol Biotechnol 93:1279–1289. https://doi.org/10.1002/jctb.5487
6. Islam MS et al (2017) Dynamics of microbial community structure and nutrient removal from an innovative side-stream enhanced biological phosphorus removal process. J Environ Manag 198:300–307. https://doi.org/10.1016/j.jenvman.2017.04.074
7. Kamika I, Azizi S, Tekere M (2018) Comparing bacterial diversity in two full-scale enhanced biological phosphate removal reactors using 16S amplicon pyrosequencing. Pol J Environ Stud 27:709–745. https://doi.org/10.15244/pjoes/69029
8. Yadav D, Anand Raja S, Pruthi V, Kumar P (2017) Enhanced biological phosphorus removal using dried powdered sludge in an aerobic baffled reactor. J Environ Eng 143:04017006. https://doi.org/10.1061/(ASCE)EE.1943-7870.0001189
9. Sumathi M, Vasudevan N (2018) Removal of phosphate by Staphylococcus aureus under aerobic and alternating anaerobic–aerobic conditions. Environ Technol 39:1071–1080. https://doi.org/10.1080/09593330.2017.1320432
10. Hashim KS et al (2019) Electrocoagulation as a green technology for phosphate removal from river water. Sep Purif Technol 210:135–144. https://doi.org/10.1016/j.seppur.2018.07.056
11. Malakootian M, Daneshkhah M, Hossaini H (2018) Removal of phosphates from aqueous solution by sepiolite-nano zero

valent iron composite optimization with response surface methodology. Int J Environ Sci Technol 15:2129–2140. https://doi.org/10.1007/s13762-017-1520-y
12. Ren X, Du C, Zhang L, Zhuang Y, Xu M (2016) Removal of phosphate in aqueous solutions by the aluminum salt slag derived from the scrap aluminum melting process. Desalin Water Treat 57:11291–11299. https://doi.org/10.1080/19443994.2015.1043956
13. Ajmal Z, Muhmood A, Usman M, Kizito S, Lu J, Dong R, Wu S (2018) Phosphate removal from aqueous solution using iron oxides: adsorption, desorption and regeneration characteristics. J Colloid Interface Sci 528:145–155. https://doi.org/10.1016/j.jcis.2018.05.084
14. Sleiman N, Deluchat V, Wazne M, Courtin A, Saad Z, Kazpard V, Baudu M (2016) Role of iron oxidation byproducts in the removal of phosphate from aqueous solution. RSC Adv 6:1627–1636. https://doi.org/10.1039/C5RA22444F
15. Son J-W et al (2016) Analysis of phosphate removal from aqueous solutions by hydrocalumite. Desalin Water Treat 57:21476–21486. https://doi.org/10.1080/19443994.2015.1119759
16. Ayoub GM, Koopman B, Pandya N (2001) Iron and aluminum hydroxy (oxide) coated filter media for low-concentration phosphorus removal. Water Environ Res 73(4):478–485
17. Fangqun G, Pinzhu Q, Guan y, Rong T, Jien H (2017) Removal of phosphate from aqueous solution using modified zeolite clays. In: IOP conference series: materials science and engineering, vol 242, p 012031
18. Mitrogiannis D et al (2017) Removal of phosphate from aqueous solutions by adsorption onto $Ca(OH)_2$ treated natural clinoptilolite. Chem Eng J 320:510–522. https://doi.org/10.1016/j.cej.2017.03.063
19. Kang J-K, Kim J-H, Kim S-B, Lee S-H, Choi J-W, Lee C-G (2016) Ammonium-functionalized mesoporous silica MCM-41 for phosphate removal from aqueous solutions. Desalin Water Treat 57:10839–10849. https://doi.org/10.1080/19443994.2015.1038590
20. Wang Y-Y, Lu H, Liu Y, Yang S (2016) Removal of phosphate from aqueous solution by SiO_2-biochar nanocomposites prepared by pyrolysis of vermiculite treated algal biomass. RSC Adv. https://doi.org/10.1039/c6ra15532d
21. Tangde VM, Prajapati SS, Mandal BB, Kulkarni NP (2017) Study of kinetics and thermodynamics of removal of phosphate from aqueous solution using activated red mud international. J Environ Res 11:39–47. https://doi.org/10.1007/s41742-017-0004-8
22. Ding W, Bai S, Mu H, Naren G (2017) Investigation of phosphate removal from aqueous solution by both coal gangues. Water Sci Technol 76:785–792. https://doi.org/10.2166/wst.2017.241
23. Cui X, Dai X, Khan KY, Li T, Yang X, He Z (2016) Removal of phosphate from aqueous solution using magnesium-alginate/chitosan modified biochar microspheres derived from Thalia dealbata. Bioresour Technol 218:1123–1132. https://doi.org/10.1016/j.biortech.2016.07.072
24. Mahaninia MH, Wilson LD (2016) Cross-linked chitosan beads for phosphate removal from aqueous solution. J Appl Polym Sci 133:5. https://doi.org/10.1002/app.42949
25. Yao S et al (2017) Removal of phosphate from aqueous solution by sewage sludge-based activated carbon loaded with pyrolusite. J Water Reuse Desalin. https://doi.org/10.2166/wrd.2017.054
26. Awual MR (2019) Efficient phosphate removal from water for controlling eutrophication using novel composite adsorbent. J Clean Prod 228:1311–1319. https://doi.org/10.1016/j.jclepro.2019.04.325
27. Awual MR, Jyo A, Ihara T, Seko N, Tamada M, Lim KT (2011) Enhanced trace phosphate removal from water by zirconium(IV) loaded fibrous adsorbent. Water Res 45:4592–4600. https://doi.org/10.1016/j.watres.2011.06.009
28. Awual MR, Shenashen MA, Yaita T, Shiwaku H, Jyo A (2012) Efficient arsenic(V) removal from water by ligand exchange fibrous adsorbent. Water Res 46:5541–5550. https://doi.org/10.1016/j.watres.2012.07.038
29. Awual R, Jyo A (2009) Rapid column-mode removal of arsenate from water by crosslinked poly(allylamine) resin. Water Res 43:1229–1236. https://doi.org/10.1016/j.watres.2008.12.018
30. Cheremisinoff NP (1993) Water treatment and waste recovery: advanced technology and applications. PTR Prentice Hall, Englewood Cliffs
31. Lee SH, Vigneswaran S, Bajracharya K (1996) Phosphorus transport in saturated slag columns: experiments and mathematical models. Water Sci Technol 34:1–2. https://doi.org/10.1016/0273-1223(96)00505-7
32. Chen D, Yu C, Bao T, Zhu C, Qing C, Chen T (2016) Simultaneous removal of nitrogen and phosphorus using autoclaved aerated concrete particles in biological aerated filters. Desalin Water Treat 57:19402–19410. https://doi.org/10.1080/19443994.2015.1096214
33. Awual MR (2016) Solid phase sensitive palladium(II) ions detection and recovery using ligand based efficient conjugate nanomaterials. Chem Eng J 300:264–272. https://doi.org/10.1016/j.cej.2016.04.071
34. Haddad F (1990) Evaluation of raw materials for the magnesia industry: selected dolomites from Southern Lebanon and Qartaba. American University of Beirut, Beirut
35. Standard Test Method for Particle-Size Analysis of Soils (2007)
36. Rice EW (2012) Standard methods for the examination of water and wastewater. American Public Health Association, Washington, DC
37. Bohart GS, Adams EQ (1920) Some aspects of the behavior of charcoal with respect to chlorin E.1. J Am Chem Soc 42:523–544. https://doi.org/10.1021/ja01448a018
38. Chu KH (2010) Fixed bed sorption: setting the record straight on the Bohart–Adams and Thomas models. J Hazard Mater 177:1006–1012. https://doi.org/10.1016/j.jhazmat.2010.01.019
39. Trgo M, Medvidović N, Peric J (2011) Application of mathematical empirical models to dynamic removal of lead on natural zeolite clinoptilolite in a fixed bed column. Indian J Chem Technol (IJCT) 18:123–131
40. Ahmad AA, Hameed BH (2010) Fixed-bed adsorption of reactive azo dye onto granular activated carbon prepared from waste. J Hazard Mater 175:298–303. https://doi.org/10.1016/j.jhazmat.2009.10.003
41. Marzbali MH, Esmaieli M (2017) Fixed bed adsorption of tetracycline on a mesoporous activated carbon: experimental study and neuro-fuzzy modeling. J Appl Res Technol 15:454–463. https://doi.org/10.1016/j.jart.2017.05.003
42. Rozada F, Otero M, García AI, Morán A (2007) Application in fixed-bed systems of adsorbents obtained from sewage sludge and discarded tyres. Dyes Pigm 72:47–56. https://doi.org/10.1016/j.dyepig.2005.07.016
43. Karunarathne HDSS, Amarasinghe BMWPK (2013) Fixed bed adsorption column studies for the removal of aqueous phenol from activated carbon prepared from sugarcane bagasse. Energy Proc 34:83–90. https://doi.org/10.1016/j.egypro.2013.06.736
44. Secor Robert M (1956) Mass-transfer operations. In: Treybal RE (ed) McGraw-Hill Book Company, Inc., New York (1955), p 666, $9.50 AIChE Journal 2:577-511D. https://doi.org/10.1002/aic.690020430
45. Chen S, Yue Q, Gao B, Li Q, Xu X, Fu K (2012) Adsorption of hexavalent chromium from aqueous solution by modified corn stalk:

a fixed-bed column study. Bioresour Technol 113:114–120. https://doi.org/10.1016/j.biortech.2011.11.110
46. Ayoob S, Gupta AK, Bhakat PB (2007) Analysis of breakthrough developments and modeling of fixed bed adsorption system for As(V) removal from water by modified calcined bauxite (MCB). Sep Purif Technol 52:430–438. https://doi.org/10.1016/j.seppur.2006.05.021
47. Yoon YH, Nelson JH (1984) Application of gas adsorption kinetics. I. A theoretical model for respirator cartridge service life. Am Ind Hyg Assoc J 45:509–516. https://doi.org/10.1080/15298668491400197
48. Awual MR, Hasan MM (2014) Novel conjugate adsorbent for visual detection and removal of toxic lead(II) ions from water. Microporous Mesoporous Mater 196:261–269. https://doi.org/10.1016/j.micromeso.2014.05.021
49. Awual MR, Hasan MM (2014) A novel fine-tuning mesoporous adsorbent for simultaneous lead(II) detection and removal from wastewater. Sens Actuat B Chem 202:395–403. https://doi.org/10.1016/j.snb.2014.05.103
50. Awual MR, Hasan MM (2015) Colorimetric detection and removal of copper(II) ions from wastewater samples using tailor-made composite adsorbent. Sens Actuat B Cheml 206:692–700. https://doi.org/10.1016/j.snb.2014.09.086
51. Awual MR, Hasan MM (2015) Fine-tuning mesoporous adsorbent for simultaneous ultra-trace palladium(II) detection, separation and recovery. J Ind Eng Chem 21:507–515. https://doi.org/10.1016/j.jiec.2014.03.013
52. Abbas K, Znad H, Awual MR (2018) A ligand anchored conjugate adsorbent for effective mercury(II) detection and removal from aqueous media. Chem Eng J 334:432–443. https://doi.org/10.1016/j.cej.2017.10.054
53. Ali M, Mian AJ, Islam MN, Awual MR, Chowdhury A (2001) Physico-mechanical properties of fabrics prepared from blends of sulphonated jute fibre with natural and synthetic fibres. Indian J Fibre Text Res (IJFTR) 26:414–417
54. Naushad M, Alothman ZA, Awual MR, Alam MM, Eldesoky GE (2015) Adsorption kinetics, isotherms, and thermodynamic studies for the adsorption of Pb 2+ and Hg 2+ metal ions from aqueous medium using Ti(IV) iodovanadate cation exchanger. Ionics 21:2237–2245. https://doi.org/10.1007/s11581-015-1401-7
55. Ayoub GM, Mehawej M (2007) Adsorption of arsenate on untreated dolomite powder. J Hazard Mater 148:259–266. https://doi.org/10.1016/j.jhazmat.2007.02.011
56. Xing B, Chen T, Liu H, Qing C, Xie J, Xie Q (2017) Removal of phosphate from aqueous solution by activated siderite ore: preparation, performance and mechanism. J Taiwan Inst Chem Eng 80:875–882. https://doi.org/10.1016/j.jtice.2017.07.016
57. Rashid M, Price NT, Gracia Pinilla MÁ, O'Shea KE (2017) Effective removal of phosphate from aqueous solution using humic acid coated magnetite nanoparticles. Water Res 123:353–360. https://doi.org/10.1016/j.watres.2017.06.085
58. Awual MR (2014) Investigation of potential conjugate adsorbent for efficient ultra-trace gold(III) detection and recovery. J Ind Eng Chem 20:3493–3501. https://doi.org/10.1016/j.jiec.2013.12.040
59. Awual MR (2015) A novel facial composite adsorbent for enhanced copper(II) detection and removal from wastewater. Chem Eng J 266:368–375. https://doi.org/10.1016/j.cej.2014.12.094
60. Awual MR (2016) Assessing of lead(III) capturing from contaminated wastewater using ligand doped conjugate adsorbent. Chem Eng J 289:65–73. https://doi.org/10.1016/j.cej.2015.12.078
61. Awual MR (2017) New type mesoporous conjugate material for selective optical copper(II) ions monitoring and removal from polluted waters. Chem Eng J 307:85–94. https://doi.org/10.1016/j.cej.2016.07.110
62. Awual MR (2016) Ring size dependent crown ether based mesoporous adsorbent for high cesium adsorption from wastewater. Chem Eng J 303:539–546. https://doi.org/10.1016/j.cej.2016.06.040
63. Awual MR (2017) Novel nanocomposite materials for efficient and selective mercury ions capturing from wastewater. Chem Eng J 307:456–465. https://doi.org/10.1016/j.cej.2016.08.108
64. Helfferich FG (1995) Ion exchange. Courier Corporation, New York
65. Xu N, Chen M, Zhou K, Wang Y, Yin H, Chen Z (2014) Retention of phosphorus on calcite and dolomite: speciation and modeling. RSC Adv 4:35205–35214. https://doi.org/10.1039/C4RA05461J
66. Karaca S, Gürses A, Ejder M, Açıkyıldız M (2006) Adsorptive removal of phosphate from aqueous solutions using raw and calcinated dolomite. J Hazard Mater 128:273–279. https://doi.org/10.1016/j.jhazmat.2005.08.003
67. Zhao D, Sengupta AK (1998) Ultimate removal of phosphate from wastewater using a new class of polymeric ion exchangers. Water Res 32:1613–1625. https://doi.org/10.1016/S0043-1354(97)00371-0
68. Guibal E, Lorenzelli R, Vincent T, Cloirec PL (1995) Application of silica gel to metal ion sorption: static and dynamic removal of uranyl ions. Environ Technol 16:101–114
69. Sekhula MM, Okonkwo JO, Zvinowanda CM, Agyei NN, Chaudhary AJ (2012) Fixed bed column adsorption of Cu(II) onto maize Tassel-PVA beads. J Chem Eng Process Technol 3:1–5. https://doi.org/10.4172/2157-7048.1000131
70. Ghribi A, Chlendi M (2011) Modeling of fixed bed adsorption: application to the adsorption of an organic dye. Asian J Text. https://doi.org/10.3923/ajt.2011.161.171